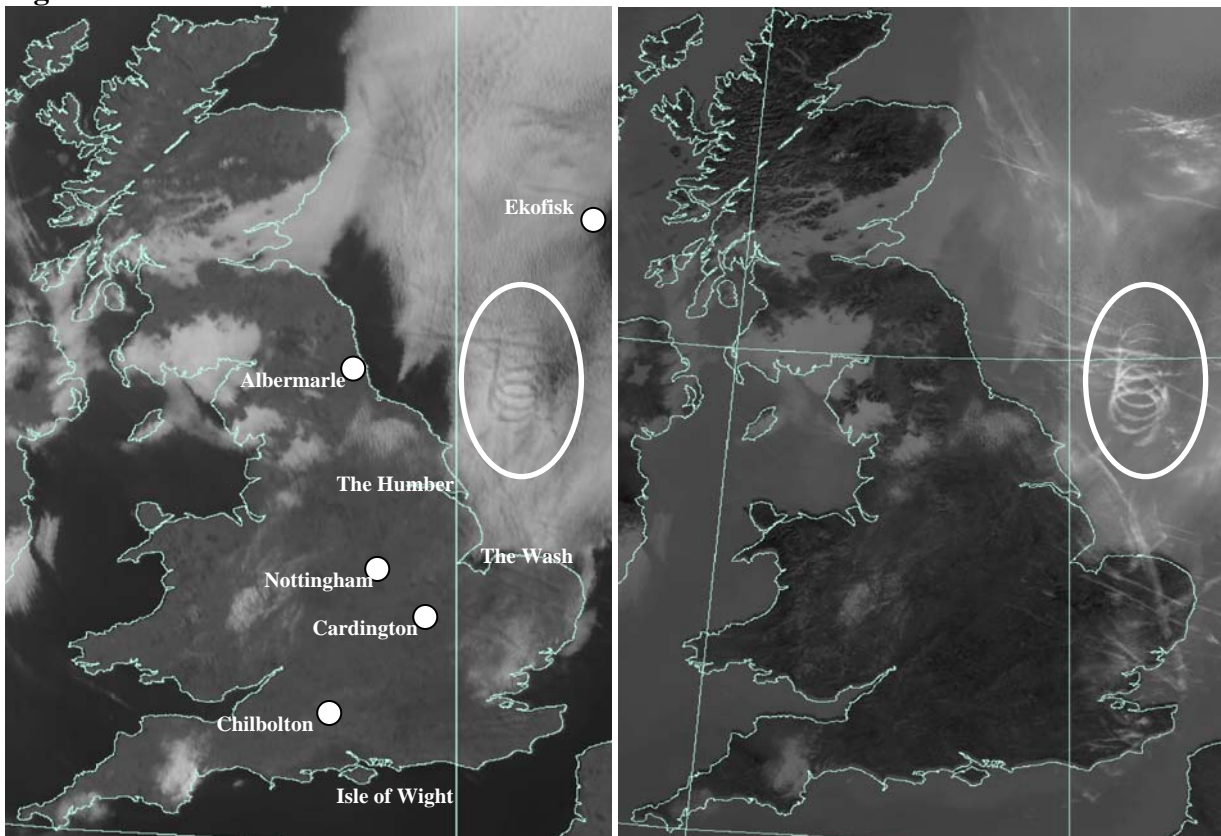
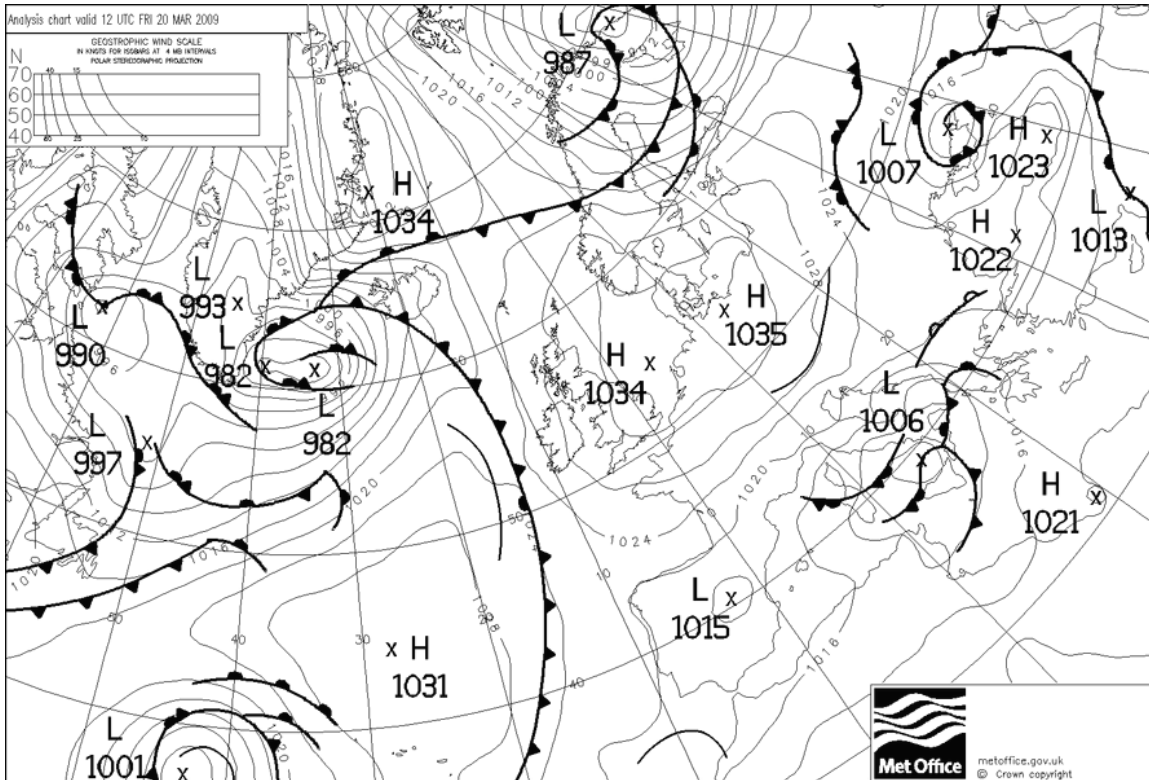


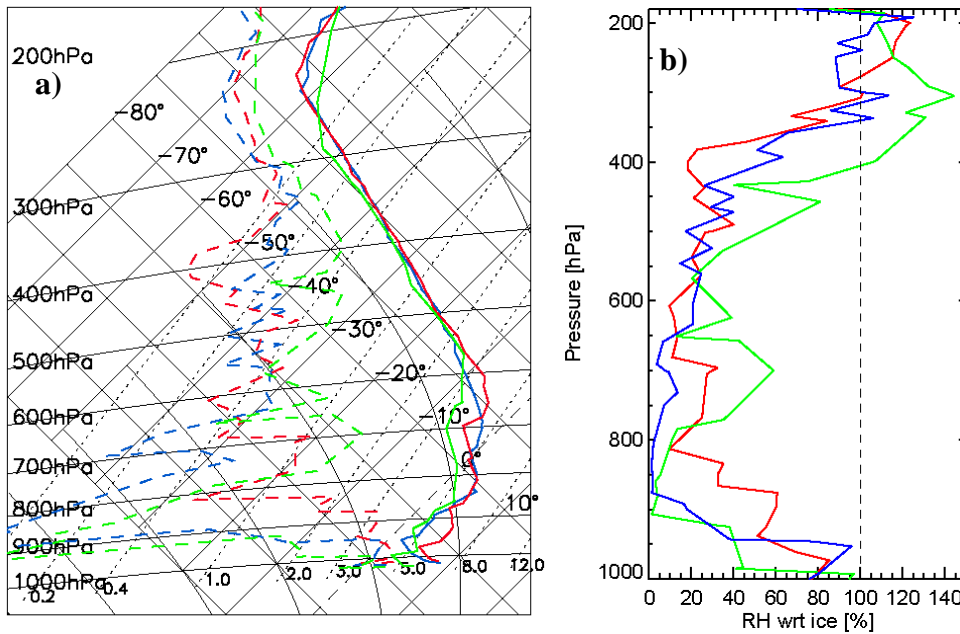
1 **Figures.**



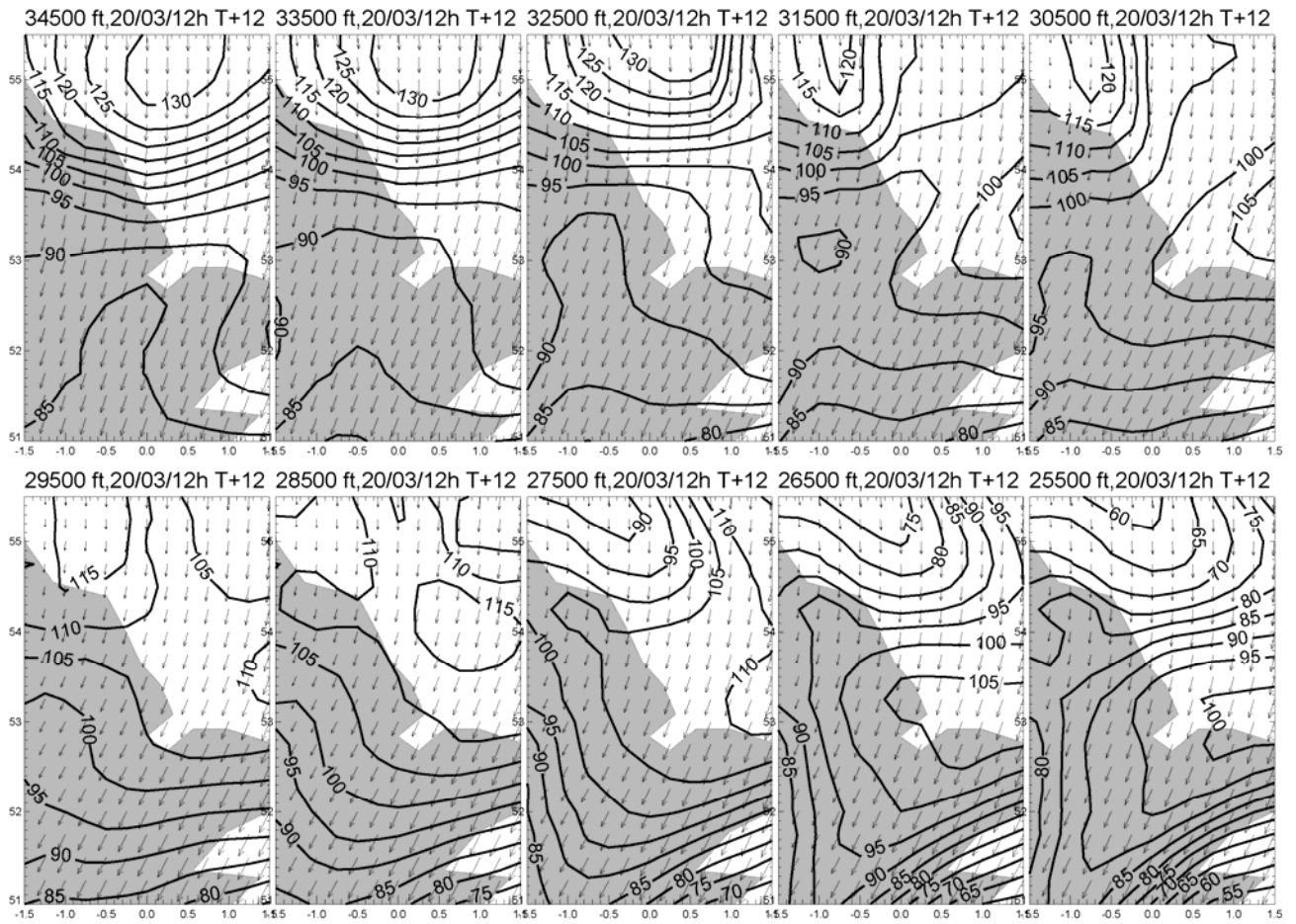
2
3 Figure 1. a) high resolution visible image ($0.65\mu\text{m}$) from the SEVIRI sensor on Meteosat-9 b) infra-red
4 ($10.8\mu\text{m}$) image obtained from the METOP satellite. Both images are from $\sim 10:40$ on 20th March 2009.
5 The white oval highlights the position of the coil-shaped contrail/cirrus (CCC). The positions of the
6 WMO radiosonde ascent sites at Nottingham, Albermarle, and Ekofisk are also shown together with the
7 approximate position of the Met Office Cardington field site, and the Chilbolton observatory.
8



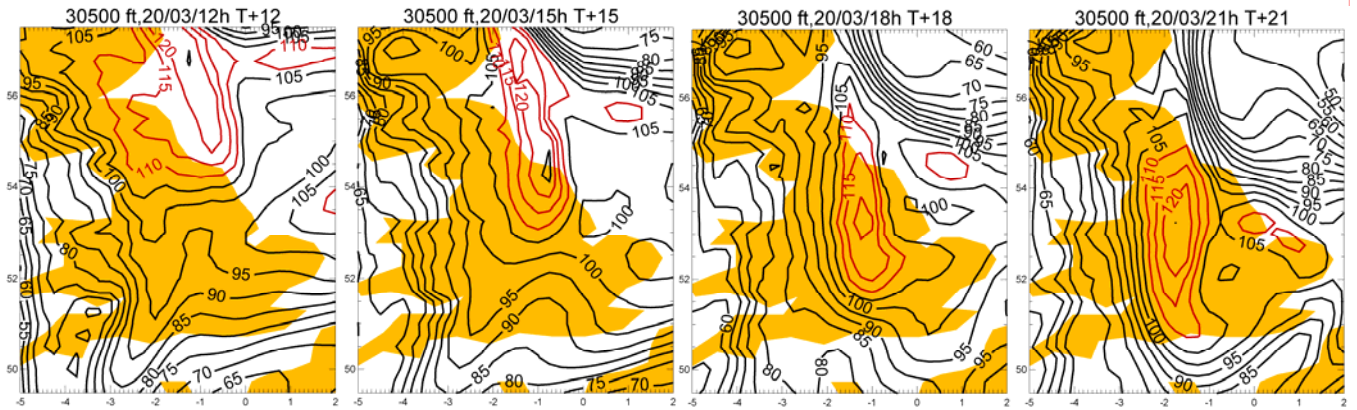
10 Figure 2. The synoptic surface analysis from the UK Met Office for 12:00 on 20 March 2009.
 11
 12
 13
 14



15 Figure 3. Tephigrams showing a) the radiosonde ascent profiles of temperature and dew point from
 16 Nottingham (blue), Albemarle (red), and Ekofisk (green) for 12:00 on March 20th 2009, b) the relative
 17 humidity with respect to ice determined from the tephigrams is shown in Figure 2b derived using the
 18 correction of *Vömel et al.* (2007).
 19

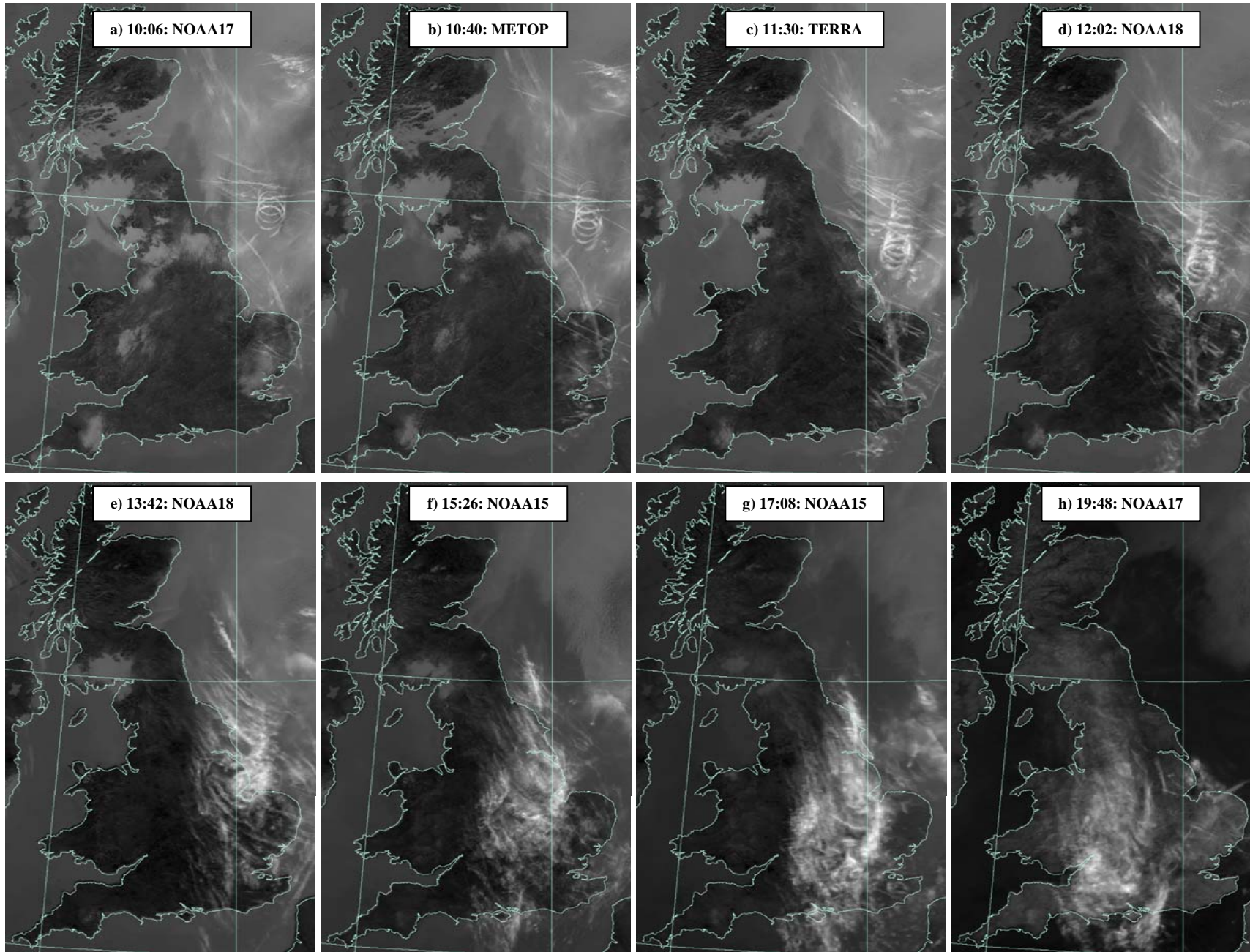


21



22

23 Figure 4. Showing the relative humidity with respect to ice over the UK derived from the ECMWF
 24 operational model. a) Altitudes from 34500ft (top left hand image) to 25500ft (bottom right hand image)
 25 and model levels every 1000ft in between. The contours show relative humidity (%), and the arrows
 26 represent wind vectors. Fields are for 12:00 on 20 March 2009 from forecasts at 00:00 on 20 March
 27 2009. b) The evolution of the supersaturated region at 30,500ft over the period 12:00-21:00. Regions
 28 with relative humidity exceeding 110% with respect to ice are contoured using red lines.



30

31

32

33

Figure 5 IR (10.8μm) images of the formation of contrail induced cirrus (bright white). Areas of stratocumulus are shown as medium grey. The time and satellite is shown in the inset in each of the frames.

34

35

36

37

38

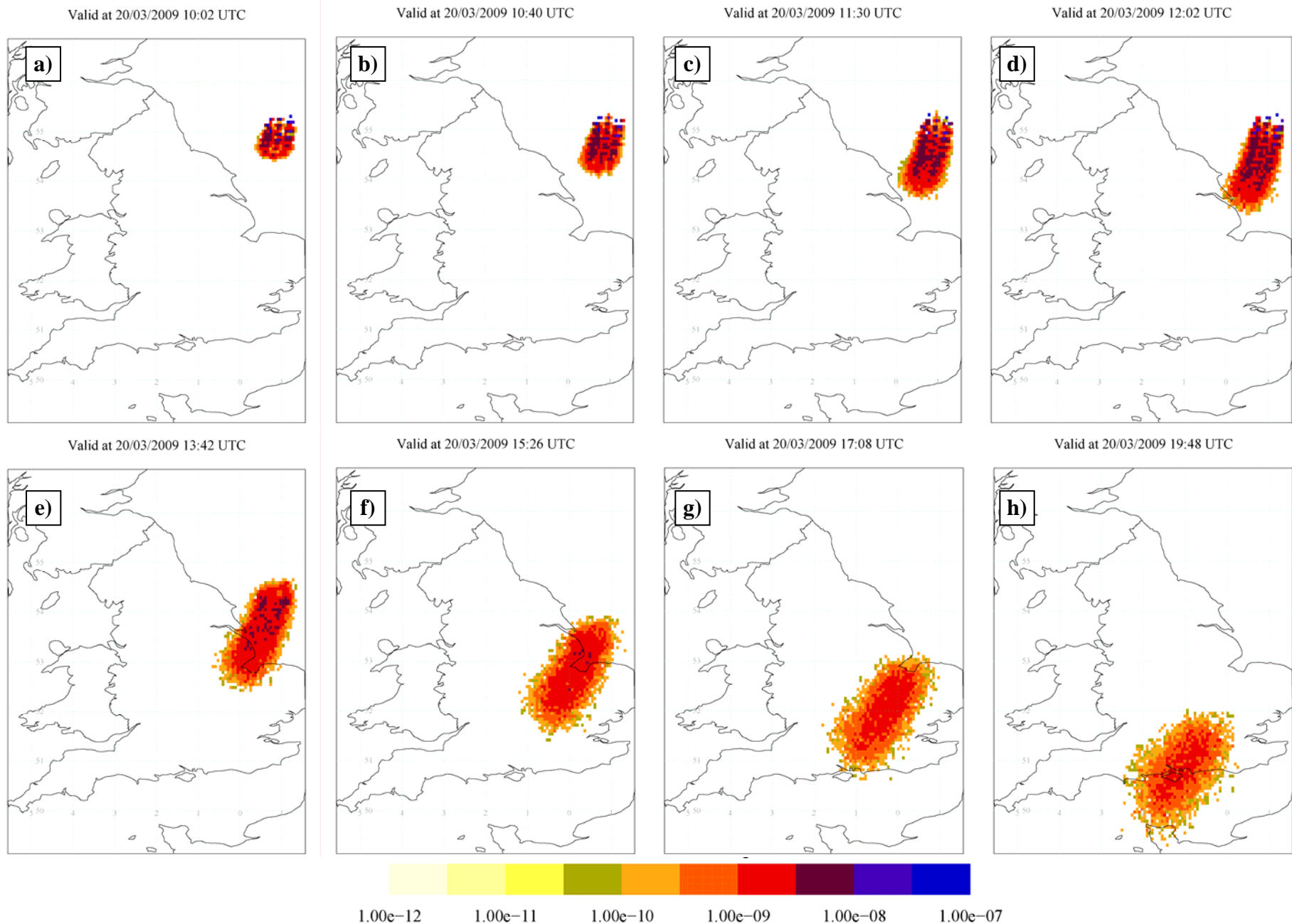
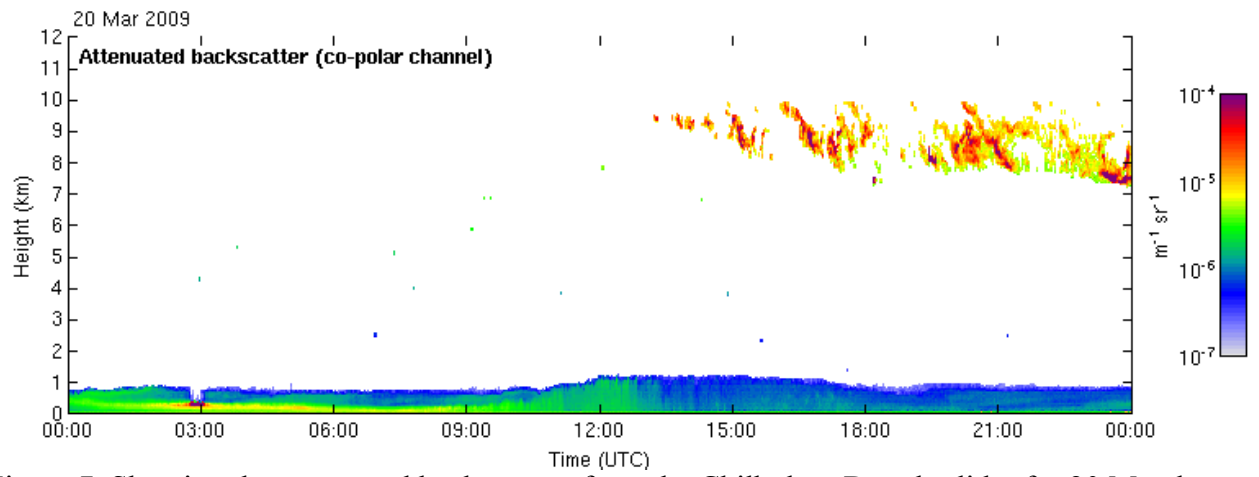


Figure 6. Results from the NAME model initiating a contrail circle at 30,000ft during the period 08:30Z to 11:50Z on 20 March 2009. The units are nominally gm^{-3} from an initial emission of 1g/second.

1



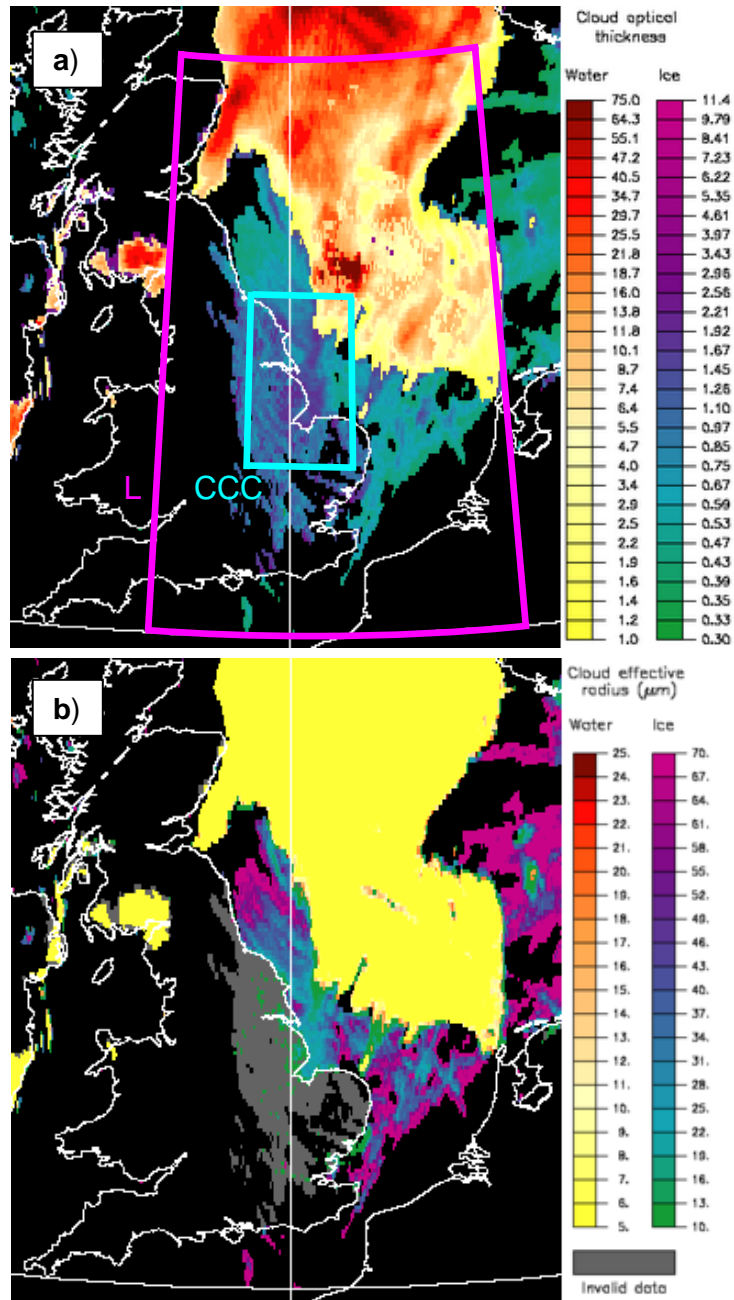
2

3

4

Figure 7. Showing the attenuated back-scatter from the Chilbolton Doppler lidar for 20 March 2009. The main altitude of contrail-induced cirrus is seen to be between 8-9km altitude.

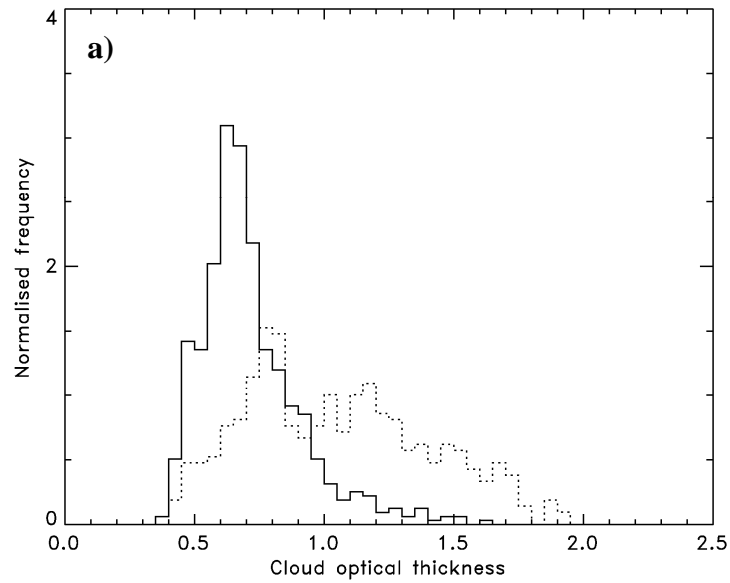
1
2



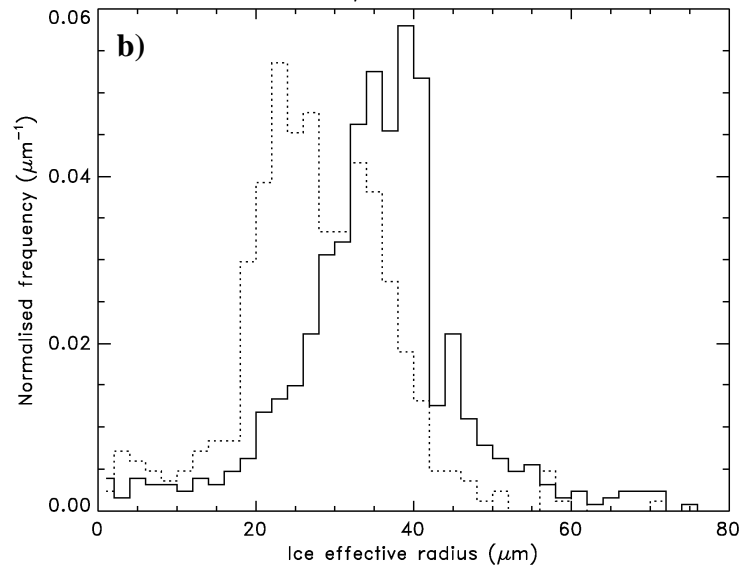
3
4
5
6
7
8
9
10
11
12
13
14
15
16
17
18
19
20
21
22
23

Figure 8. Retrievals of the a) visible ($\sim 0.55\mu\text{m}$) cloud optical thickness, b) effective radius (μm) for 14:00 on 20 March 2009. The two scales on each plot are for water cloud and for ice cloud respectively. The coil-shaped contrail/cirrus (CCC) and larger (L) areas referred to in the text are shown in a) as cyan and magenta boxes respectively.

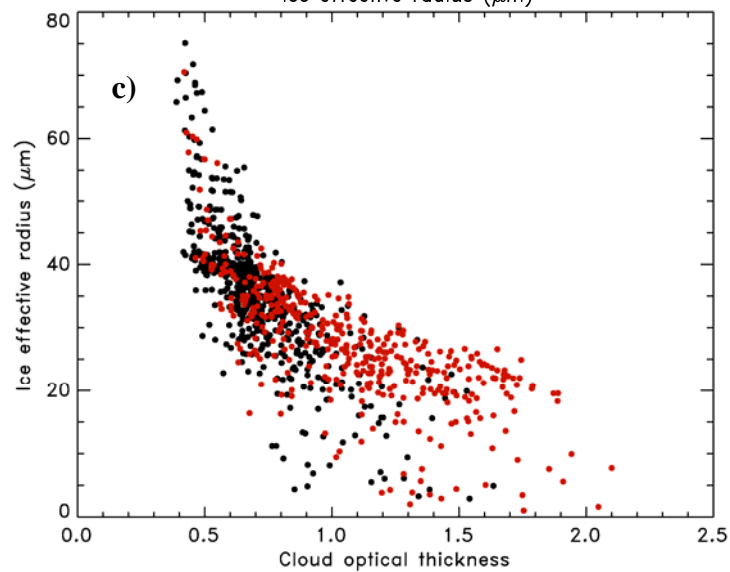
1



2



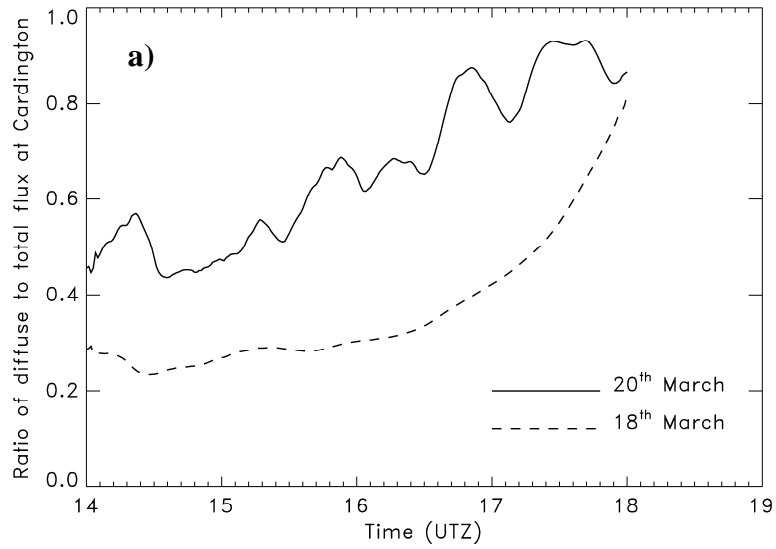
3



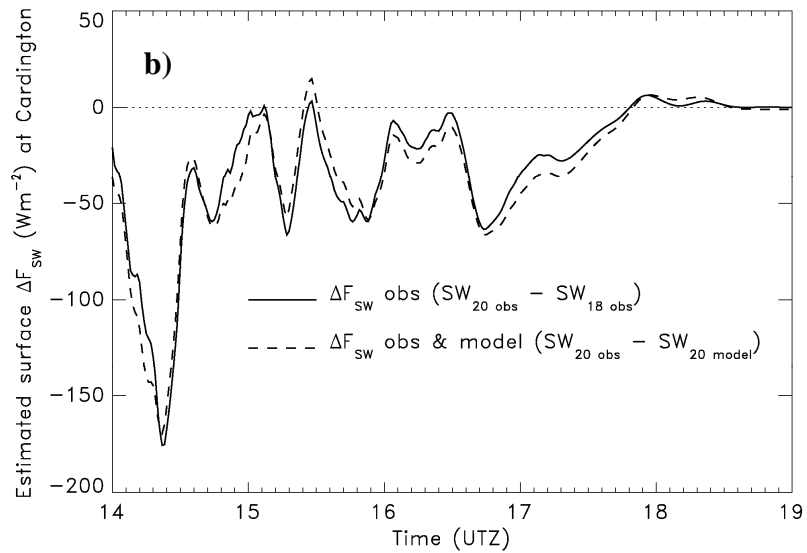
4

5 Figure 9. Frequency distributions of a) the cloud optical depth, b) cloud top ice effective radius at
6 14:00. For each plot, the solid line shows the ice cloud properties derived over the residual area
7 (i.e. L minus CCC), while the dotted line shows properties derived for the CCC area. c) shows a
8 scatter plot of the ice effective radius against the cloud optical thickness. Black dots indicate points
9 from the residual area, and red from the CCC area.

1



2



3

4

5

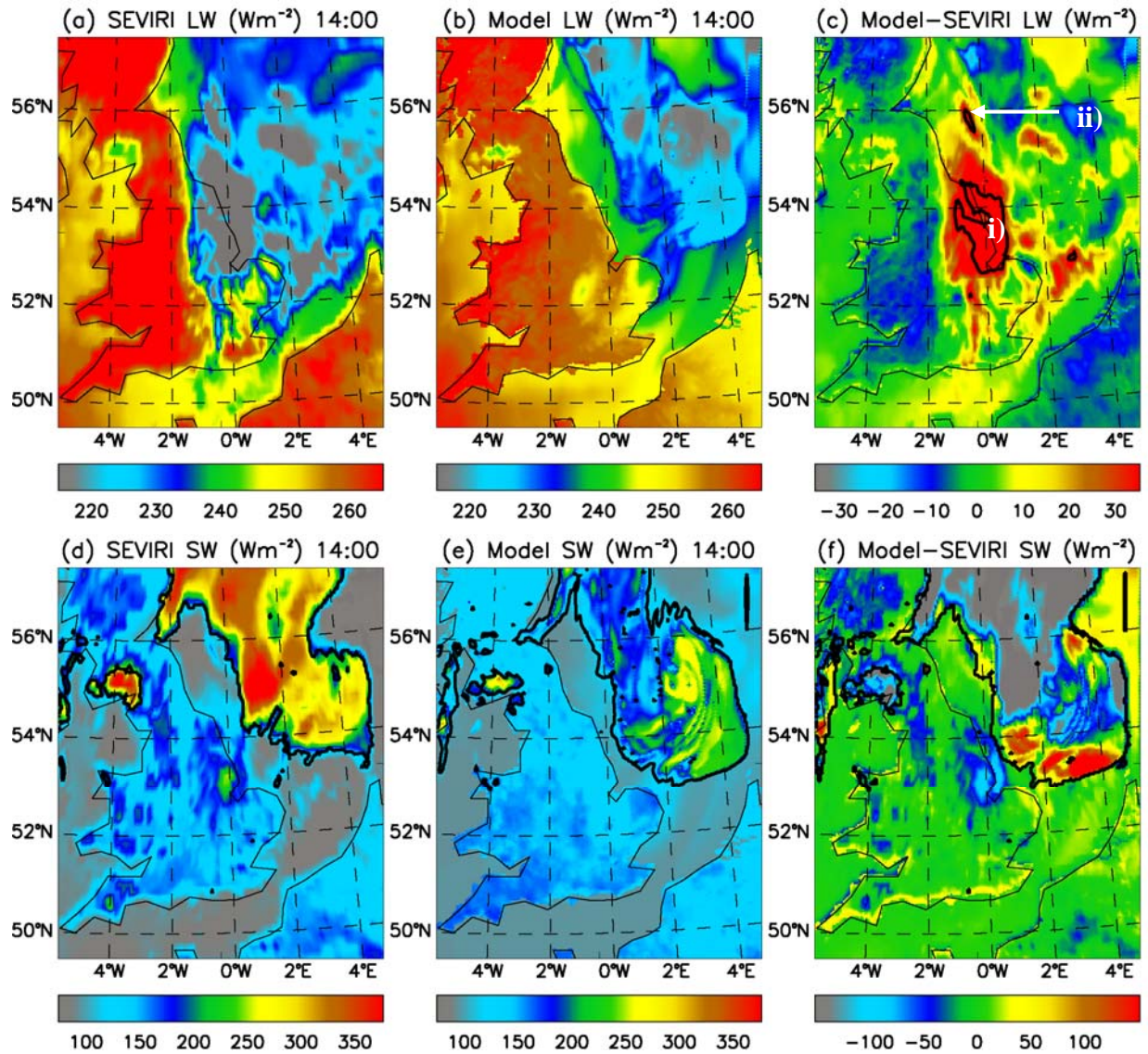
6

7

8

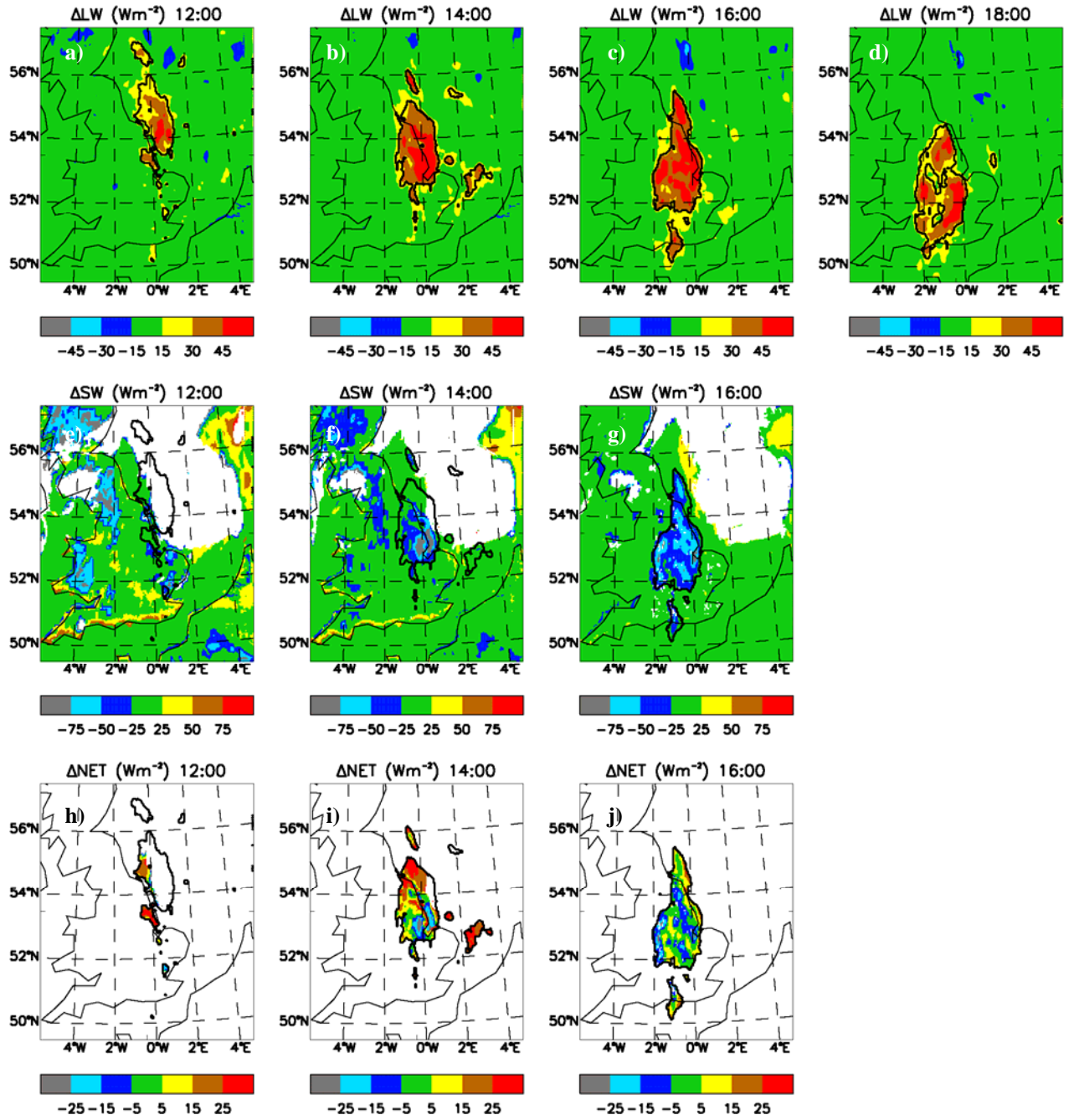
9

Figure 10. Showing the a) ratio of diffuse to total downward solar irradiance for the 20 March 2009 (contrail case) and for the 18 March 2009 (no contrails), b) the estimated change in the downward surface irradiance (Wm^{-2}) at Cardington derived using two different methods (see text for details).



1
2
3
4
5
6
7
8
9

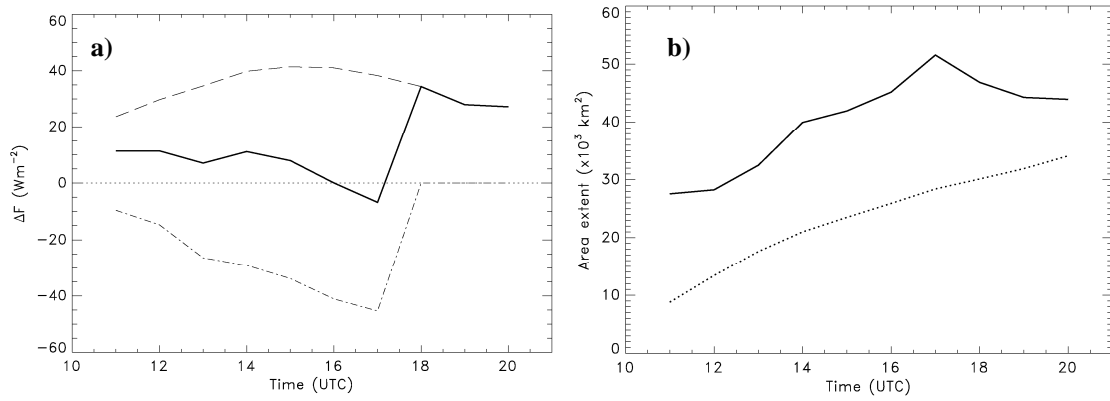
Figure 11. Showing a) $LW_{\uparrow satellite}$, b) $LW_{\uparrow model}$, c) ΔF_{LW_TOA} , d) $SW_{\uparrow satellite}$, e) $SW_{\uparrow model}$, and f) ΔF_{SW_TOA} for the top of the atmosphere for 14:00Z for March 20th, 2009. In c), the contour interval represents $\Delta F_{LW_TOA} > 40 Wm^{-2}$. In d), e) and f), the contour encompasses areas of liquid water cloud (see text for details of the cloud screening procedure).



1
2
3
4
5
6

Figure 12. Showing a-d) the evolution of ΔF_{LW_TOA} , e-g) ΔF_{SW_TOA} , and h-j) ΔF_{net_TOA} on the 20 March 2010. The contour interval marked on the figures shows areas defined as contrail as described in the text.

1



2

3

4

5

6

Figure 13. a) $\Delta F_{\text{LW_TOA}}$, $\Delta F_{\text{SW_TOA}}$, and $\Delta F_{\text{net_TOA}}$ determined in the area marked by the solid contour on Figure 12 as described in the text. b) The areal extent of the contrail-induced cirrus (in 1000s of km^2) determined from $\Delta F_{\text{LW_TOA}}$ (solid line) and for the CCC determined from the NAME model (dotted line) as a function of time.